Gold sensitized sprayed SnO_2 nanostructured film for enhanced LPG sensing

Umesh T. Nakate[a,d,*], Pramila Patil[b], Balaji G. Ghule[d], Satish Ekar[d], Ahmed Al-Osta[d], V.V. Jadhav[c], Rajaram S. Mane[d,e,*], S.N. Kale[a], Mu. Naushad[e], Colm O'Dwyer[f]

[a] *Thin Films Laboratory, Department of Applied Physics, Defence Institute of Advanced Technology (Deemed University), Girinagar, Pune – 411025, Maharashtra, India*

[b] *Defence Bioengineering and Electromedical Laboratory, Bangalore – 560093, Karnataka, India*

[c] *Department of Physics, Shivaji Mahavidyalya, Udgir, Dist Latur, M.S., India*

[d] *Centre for Nano-Materials & Energy Devices, School of Physical Sciences, Swami Ramanand Teerth Marathwada University, Nanded – 431606, M.S., India*

[e] *Department of Chemistry, College of Science, King Saud University, Bld#5, Riyadh, Saudi Arabia*

[f] *School of Chemistry, University College of Cork, Cork, Ireland*

Abstract

We report LPG sensing of gold (Au)-sensitized SnO_2 nanostructured film fabricated by an easy spray pyrolysis deposition method whose surface morphology is confirmed by field-emission scanning elec- tron microscopy and atomic force microscopy images and structure by X-ray diffraction pattern. Energy dispersive X-ray spectrometer analysis has carried out for finding elemental composition. The SnO_2 film is uniform and consists of spherical particles of ~10 nm. The highest gas response observed at 780 ppm LPG concentration for pristine SnO_2 is 28%, at operating temperature 623 K, which is greatly improved on Au sensitization up to 57% with 60 s rapid response time at 598 K operating temperarture. The high gas response is due to electronic effect and catalytic spill-over effect of Au sensitization. The improved sensing mechanism has throughly been explored .

1. **Introduction**

The detection of inflammable and explosive gases has become an important area of research. The leakage of these gases can cause major explosions/accidents. The LPG, one of the highly inflammable and potentially hazardous gases is widely used in household, vehicle fuels and at the industry level. Nowadays accidents due leakage of LPG are significantly increasing. The accidental leakage of LPG has been increased awareness for efficient detection and constant monitoring. Taking into the account, there is need for high sensitivity and low concentration level detection of LPG. The nanocrystalline semiconducting metal oxide resistive gas sensors have attracted great attention for a long time, due to their low costs, ease of fabrication and high sensitivity towards various oxidizing and reducing gases [1]. The metal oxides like SnO_2 [2], TiO_2 [3], ZnO [4], and CdO [5] have been envisaged for gas sensing application. The SnO_2 is one of the most promising materials that has been used as a gas sensor for the detection of a variety of gases [6]. Under the given operation conditions, SnO_2 based gas sensors find good chemical and thermal stabilities along with high mobility of conduction electrons [7]. The SnO_2 is most practically used device due to its excellent inherent property of the exchange of oxygen with atmosphere [8–10]. It is reported that gas sensitivity can be enhanced using the metal catalytic effect of noble metals like gold (Au) [11,12], platinum (Pt) [13–15], and palladium (Pd) [16–18]. The methods used for noble metal doping or surface sensitization/functionalization increases gas sensing performance. There is need of developing new methods for sensitization/functionalization of noble metal nanoparticles to improve gas sensing properties. Several methods have been followed for deposition of SnO_2 films such as aerosol-assisted chemical vapour deposition [19], pulsed laser deposition [20], RF sputtering [21], physical vapour deposition [22] etc. Spray pyrolysis deposition (SPD) has advantages such as it is very simple, economical, and no vacuum required, free from the high quality substrates or chemicals, formation of denser and porous films [23,24]. The Au sensitizated SnO_2 film is prepared by SPD method. This Au sensitized SnO_2 film has evidenced enhanced LPG sensing properties in comparison with pristine SnO_2 film. In the present study, Au sensi-

tized SnO_2 films have used for LPG sensing properties. Synthesis of SnO_2 films (using stannic tetrachloride solution) with Au sensitization have done by SPD method. The nanostructured SnO_2 films, with and without Au-sensitization, have characterized for their morphologies; crystal structures and sensitization measurements. The LPG sensing responses for different operating temperatures and LPG concentrations are studied. Sensor stability is recorded. The transient response for LPG has also studied. The probable mechanism for enhancement in LPG sensing is discussed using schematics and band diagram.

2. Experimental

The SnO_2 films were deposited on glass substrate by SPD method using 0.3 M solution of stannic tetrachloride. The molar solution of stannic tetrachloride salt was prepared in the solvent i.e. distilled water: methanol (ratio 2:3). The prepared solution sprayed through a steel nozzle on to the ultrasonically cleaned glass substrate at 675 K. The distance between nozzle and glass substrate was fixed at 25 cm with 3 ml/min spray rate using air as the carrier gas. The temperature of glass substrates was controlled by using electronic PID temperature controller unit. The hazardous fumes generated from thermal decomposition of solution were expelled out via the exhaust. Deposited films were kept for 1 h on heater at deposition temperature to provide an additional crystallization. Au sensitization was done on the surface of SnO_2 using 0.001 M solution of $HAuCl_4 \cdot H_2O$ aqueous solution at 523 K by SPD method. All depositions were done by using Holmarc Opto-Mechatronics PVT. LTD. SPD system (model No. HO-TH-04). The Au sensitized and pure SnO_2 samples were used for their structural, morphological and optical properties initially and then employed for LPG sensing properties.

The phase formation of the SnO_2 sample was confirmed using X-ray diffractometer (XRD) with Cu-Kα (wavelength = 1.5406 Å) radiation in the 2θ range from 20 to 80°. Morphology of pristine and sensitized SnO_2 films was confirmed using field-emission scanning electron microscope (FE-SEM) and atomic force microscopy (AFM) digital images. Elemental composition was recorded by energy dispersive X-ray spectroscopy (EDS). To measure gas sensing properties, silver paint contacts with two copper rod electrodes on both films were fixed for electrical measurements. The test sample was kept in a sealed chamber and stabilized resistivity (R_a) of the SnO_2 film in the air was measured. Thereafter, LPG gas was injected into the chamber and resistivity of the sample after allowing sufficient time for equilibrium in the presence of LPG gas (R_g) was recorded. Since test chamber was sealed by keeping other gas sensing parameters constant, the change in resistivity of the sample was monitored on account of LPG exposure. The gas response formula used for sensor sensitivity measurement followed [5]

$$S = ((R_a - R_g)/R_a) \times 100\%. \quad (1)$$

The LPG sensing properties were studied by using a computer controlled system.

3. Results and discussions

3.1. Structural analysis

The X-ray diffraction patterns for SnO_2 and Au-SnO_2 films are as shown in Fig. 1. Peaks in pattern reveal confirmation of SnO_2 crystal structure [25]. The XRD peaks are also matched with standard PCPDF data PDF#721147, which confirms SnO_2 tetragonal structure. XRD peaks are sharp with good intensity, which shows high crystallinity and purity of SnO_2 sample however, peaks for Au in Au-SnO_2 XRD pattern are missing, this may be because of involvement

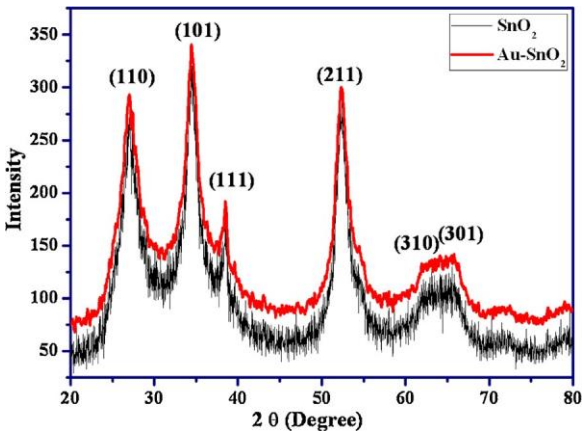

Fig. 1. The XRD patterns of the SnO_2 and Au-SnO_2 films.

of very less concentration of Au salt (0.001 M) used while sensitization as a result there are quite less number of Au nanoparticles on SnO_2 film. The less number of Au nanoparticles may not contribute in XRD pattern. The crystallite size of $SnO_2$was calculated using Scherrer's formula as [26].

$$D = \frac{K\lambda}{\beta Cos\theta} \quad (2)$$

where, λ is the wavelength of X-ray, β is the full width and half maxima, θ is the Bragg's angle. The average crystallite size is estimated to be ~6 nm from the most intensive peak of XRD spectrum. The broad peaks in XRD pattern confirm smaller crystallite size of the SnO_2 film.

3.2. Morphological and elemental analysis studies

The two-dimensional (2-D) SnO_2 morphology studies have been carried out using FE-SEM. The FE-SEM micrograph images for SnO_2 and Au sensitized SnO_2 are shown in Fig. 2 a) and b), respectively. The spherical particle-like morphology with diameter below 10 nm is evidenced from Fig. 2a) which can provide the high surface to volume ratio by allowing a maximum number of surface atoms to participate in gas sensing reaction. The particles are observed to be arranged in a highly uniform fashion and the morphology of nanoparticles predicts high adsorption of the target gas, which may help in getting more response/sensitivity. The water contact angle image of SnO_2 film recorded is given as an inset of Fig. 2. The SnO_2 film with 96° water contact angle confirms hydrophobic nature (96° > 90°).

The three-dimensional (3-D) AFM images of SnO_2 and Au-SnO_2 surfaces were recorded (Fig. 3). The spherical-type morphology of SnO_2 sample is confirmed by AFM image. The AFM image exhibits 7 nm root mean square roughness (R_q) and 5 nm arithmetic average roughness (R_a) for SnO_2 sample whereas R_q is 10 and R_a is 8 nm for Au-SnO_2 sample. Au-SnO_2 film surface is rougher than SnO_2 which may be attributed to the presence of Au nanoparticles. Morphology and surface roughness affect on the gas sensing performance since different morphologies and different surface roughnesses offer different surface areas which provide active sites for gas adsorption and hence sensing output.

To confirm the noble metal sensitization on metal oxide sensing film, the EDS measurements were carried out at various places of sensor surface [5]. The quantitative analysis of EDS spectrum for sensitized film sample shows the presence of Sn, O and Au elements (Fig. 4). The atomic percentages of Sn, O and Au are found to be 23.74, 94.85 and 1.40, respectively. The high concentration of oxygen (O) is due to the stoichiometric ratio of Sn:O (1:2). The concentration of noble metal salt (Au) used in present work for sen-

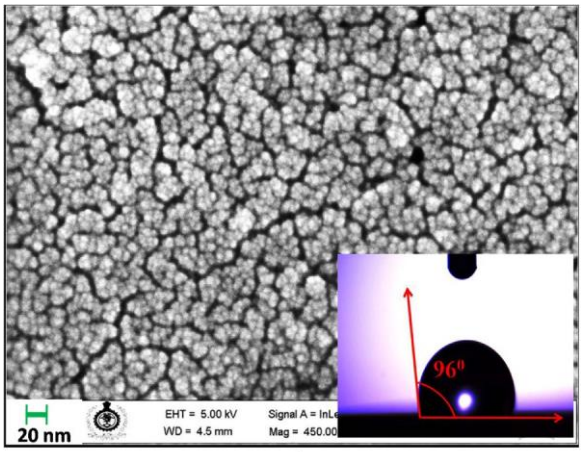

a)

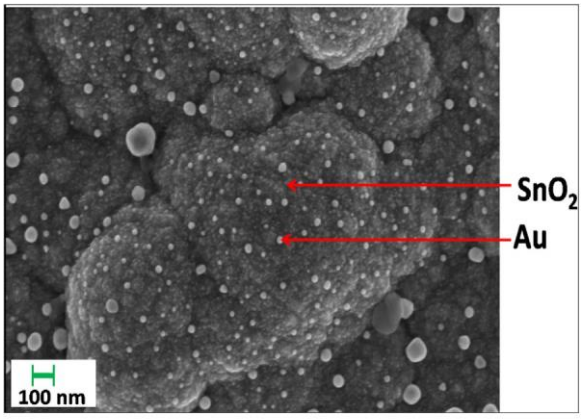

b)

Fig. 2. The field emission scanning electron micrograph images of; a) SnO_2 and b) Au sensitized SnO_2 films(respective surface contact angle measurement image as inset).

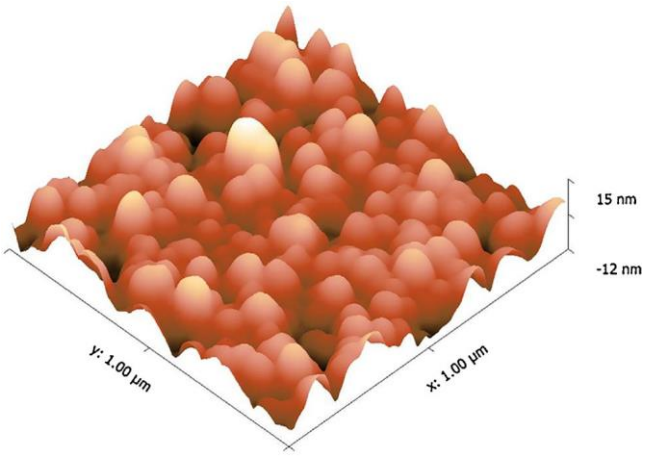

a)

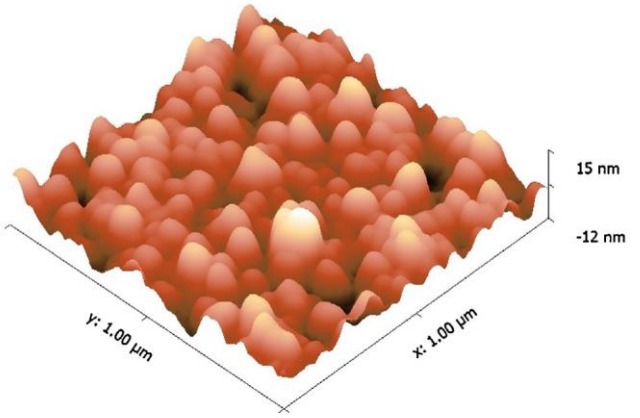

b)

Fig. 3. Three-dimensional AFM images of; a) SnO_2 and, b) Au sensitized SnO_2 films.

sitization was 0.001 M (1 mM), which is much lesser compared to noble metal (Pd) used for sensitization in previous report[5]. The presence of Au on/in the SnO_2 film surface is thus confirmed . Au nanoparticles and their cluster on the surface of SnO_2 film can be observed from FE-SEM image (Fig. 2 b). Average Au nanoparticle size is measured to be ~14 nm. The presence of Au nanoparticles on SnO_2 film can also be confirmed by UV-absorbance spectrum which is the inset of Fig. 4. The characteristic plasmon resonance absorbance peak of Au nanoparticles (533 nm) along with SnO_2 absorbance peak is observed in UV absorbance spectrum of Au sensitized SnO_2 film.

3.3. *Optical properties*

The band gaps of SnO_2 and Au-SnO_2 films were calculated from Tauc's plots. The Tauc's relation of photon energy ($h\nu$) with absorption coefficient (α) is given as [4]

$$\alpha = \frac{\alpha_0(h\nu - E_g)^n}{h\nu} \tag{3}$$

where, E_g is the band gap of material, $h\nu$ is the photon energy, α is absorption coefficient, α_0 is constant. The value of 'n' depends upon the transition type. The 'n' can have values 1/2, 3/2, 2 and 3 for direct allowed, direct forbidden, indirect allowed and indirect forbidden transitions, respectively. The Tauc's plots are shown in Fig. 5. The linear absorption edge confirms direct band gap with

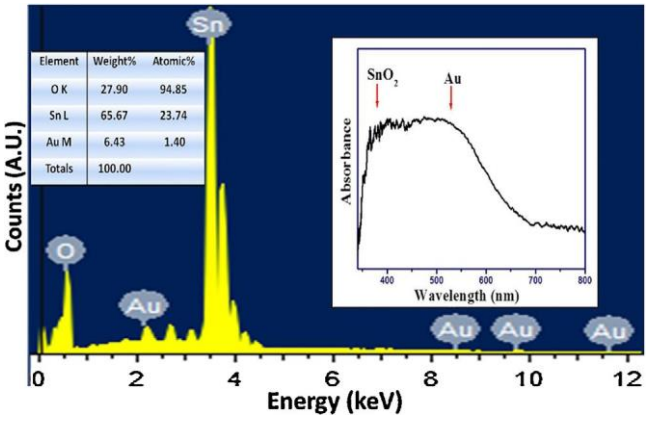

Fig. 4. EDS spectrum of Au sensitized SnO_2 film(with inset as UV-absorbance).

semiconducting nature of SnO_2 film. By extrapolating straight line portion up to photon energy axis (X-axis in Tauc's plot Fig. 5) to zero which corresponds to zero absorption coefficient value gives band gap. The band gap values for SnO_2 and Au-SnO_2 are estimated to be 3.2 eV and 3.15 eV, respectively. The lesser band gap of Au-SnO_2 may be attributed to the presence of Au nanoparticles, which creates allowed energy levels in between Fermi energy and conduction band of materials. The activation energy required for lesser band

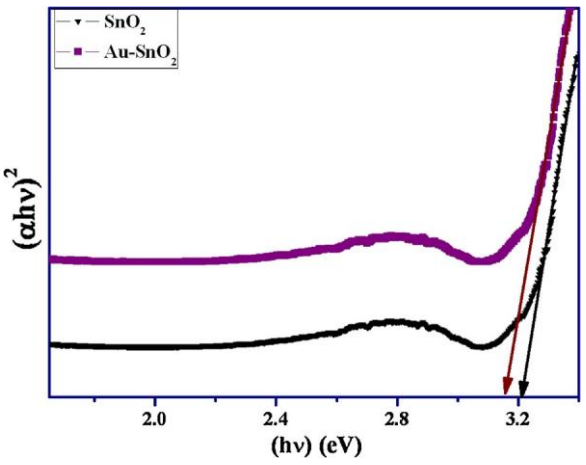

Fig. 5. Tauc's plots for SnO_2 and Au-SnO_2 films.

gap materials is less. This may lead to develop smaller operating temperature for said sensor. At lower operating temperature there is a high rate of gas adsorption and hence sensing performance can be the function of band gap energy.

3.4. *LPG sensing properties*

The LPG responses of pure SnO_2 and Au sensitized SnO_2 films as a function of operating temperature are shown in Fig. 6a) at the exposure of 520 ppm LPG concentration. The LPG response for unsensitized SnO_2 is increased up to 26% with increase in temperature up to 623 K and further it is decreased at 675 K, whereas for Au -sensitized SnO_2, a maximum response of 32% at relatively low temperature 598 K is achieved. The optimal working temperatures for SnO_2 and Au-sensitized SnO_2 films are found out to be 623 K and 598 K, respectively.

At low operation temperatures, gas molecules do not have enough thermal energy to react with the surface chemisorbed oxygen species, which results in low LPG response. The chemisorbed oxygen draws electrons from the conduction band of SnO_2 and a potential barrier to charge transport is developed. The potential barrier can be overcome due to the sufficient thermal energy obtained at higher temperatures, and sensing reaction leads to significant increase in the electron concentration. The gas response of a semiconductor metal oxide gas sensors depends on the speed of the surface chemical reaction of the crystallites and the diffusion speed of the gas molecules at the surface enhances. Since activation energy of gas sensing chemical reaction is higher, the higher temperature is required.

The LPG sensing response at lower temperatures is restricted by the speed of the chemical reaction; it is restricted by the gas molecules diffusion speed at higher temperatures. The speed of chemical reaction and gas diffusion processes become equal at some intermediate temperature, and at that point, the sensor response reaches its maximum [27]. That intermediate operating temperature for unsensitized SnO_2 is 623 K and for Au surface sensitized SnO_2 film is 598 K. The selectivities of SnO_2 and Au-SnO_2 sensors toward LPG are given in Fig. 6b. As compared to other gases, the present sensor is observed to be quite selective.

3.5. *LPG sensing mechanism for SnO_2 and Au-sensitized SnO_2*

The gas sensing properties of metal oxide depend on the various process such as adsorption, desorption, and diffusion of gases inside crystal lattice. The LPG sensing mechanism is surface controlled; change in the resistance is controlled by the charged species and

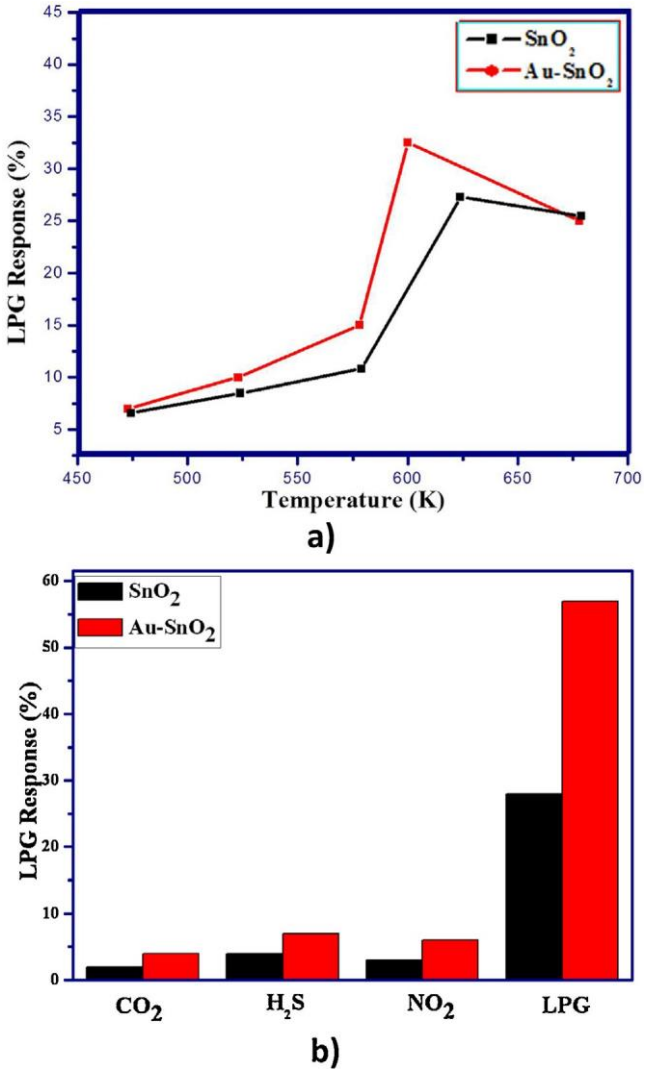

Fig. 6. a) LPG responses of the SnO_2 film and Au sensitized SnO_2 films upon exposure to 520 ppm of LPG at various temperatures. b) selectivity graphs for SnO_2 and Au-SnO_2 films.

amount of chemisorbed oxygen on the surface. The mechanism of LPG reaction proceeds through several intermediate steps and quite complex, which has not yet fully understood [28]. Prior to exposure of LPG, air oxygen gets adsorbed on the sensor surface at an operating temperature and draws electrons from the conduction band of the sensor material [29], that can be explained by the following reactions (4)–(6) [30]:

$$O_{2(gas)} \rightarrow O_{2(ads)} \quad (4)$$

$$O_{2(ads)} + e- \rightarrow (SnO_2)O_{2(ads)}- \quad (5)$$

$$O_{2(ads)}- + e- \rightarrow 2O_{(ads)}- \quad (6)$$

After saturation of the chemisorbed oxygen, the surface resistance of sensor martial stabilizes. The electrical property or resistance of the sensing film changes due to any chemical reduction or oxidation process happens on sensor surface [29]. The LPG consists of hydrocarbons like CH_4, C_3H_8,C_4H_{10}, etc., and in these molecules, the reducing hydrogen species are bound to carbon atoms. Therefore, LPG dissociates less easily into reactive reducing components on the metal oxide surface. The overall reaction of

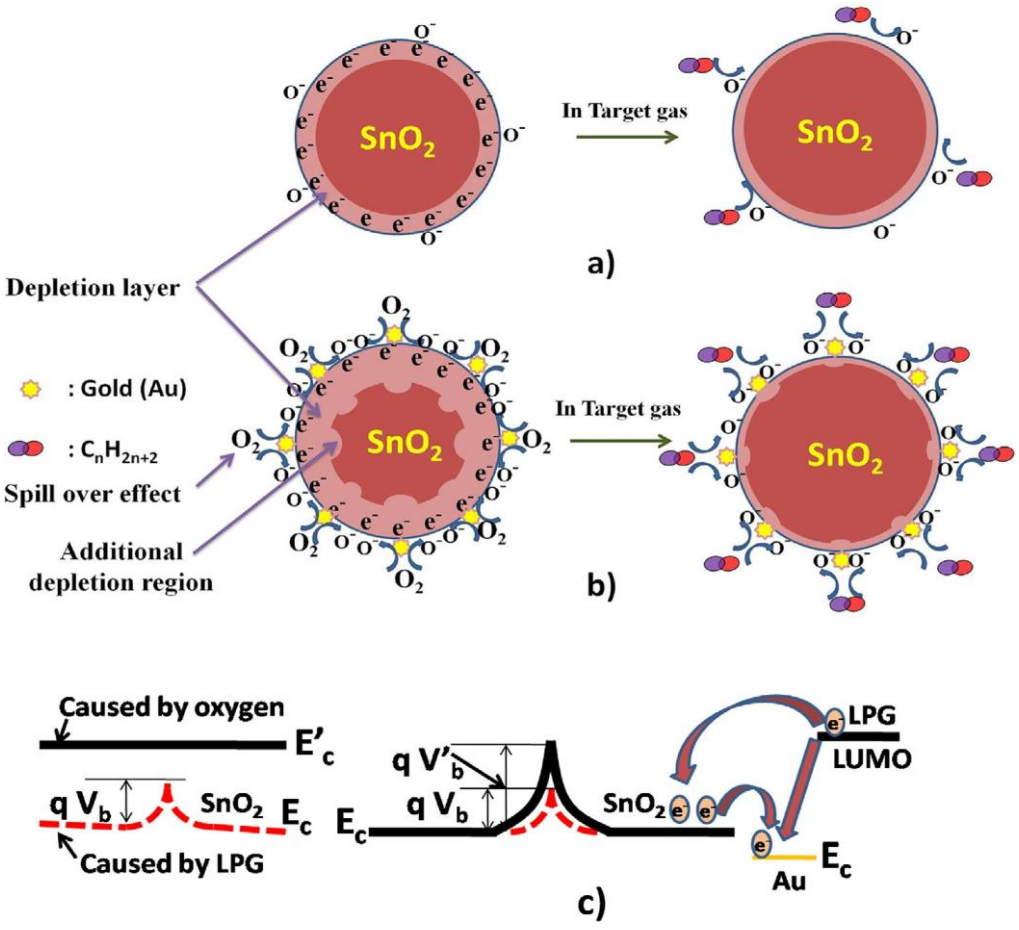

Fig. 7. Schematic diagram of LPG sensing mechanism of; a) unsensitized, b) Au-sensitized SnO_2 films, c) band structure change of sensor system on Au-sensitization.

LPG molecules with adsorbed oxygen can be explained as follows [27]:

$$C_nH_{2n+2} + 2O_{(ads)}^{-} \rightarrow H_2O + C_nH_{2n}{:}\,O + e- \quad (7)$$

$$C_nH_{2n}{:}\,O + O_{(ads)}^{-} \rightarrow CO_2 + H_2O + e- \quad (8)$$

where, C_nH_{2n+2} represent the CH_4, C_3H_8 and C_4H_{10} and C_nH_{2n}:O represent partially oxidized intermediates on the SnO_2 surface. This reaction gives product CO_2, H_2O and releases electrons back to the conduction band of sensing material, hence the resistance of the sensing material decreases with the exposure of LPG.

Noble metals are intentionally introduced to promote the receptor function and thus improve the sensing behaviours in terms of response, response/recovery times and selectivity for certain gases [31]. The metal catalytic additive increases the specific reac- tions rate on the metal oxide grain surface via modification of surface energy states and spill-over mechanism. The effects of the noble metals on the improvement of sensor response follow two types of mechanisms i.e. electric effect [32] and chemical effect [33,34]. A possible mechanism for enhancement in LPG response is schematically shown in Fig. 7. For the unsensitized SnO_2 film, Au nanoparticles on the surface are missing, chemisorbed oxygen molecules draw electrons from the SnO_2 so that it creates an electron depleted layer beneath the surface of SnO_2 nanoparticles(Fig. 7a). With the LPG exposure, oxygen concentration decreases, this suppresses the growth of electron depleted layer width. Whereas in the case of Au sensitized SnO_2 film, the change in electron depleted layer width is more remarkable due to electric and catalytic chemical effects during the exposure of LPG, and hence great enhancement in response towards LPG sensing is observed. The electronic effect is associated with the creation of electron-depleted regions beneath the Au particles due to the flow of electrons from the conduction band of SnO_2 to Au particle; consequently increases an additional electron-depleted region. In electron-depleted region state Au particles on the surface of SnO_2 provides more active sites for oxygen adsorption and enhance the migration of adsorbed oxygen molecules onto SnO_2, which are less likely to adsorb oxygen molecules. Due to this spillover effect, the adsorption of oxygen species will be facilitated, which leads to increase in thickness of the electron-depleted layer, and flow of electrons in the underlying conduction channel will be significantly more suppressed(Fig. 7b). The similar explanation of schematic sensing mechanism for noble metal sensitized gas sensors has reported earlier [11,14]. The exposure of LPG readily expands the width of conduction channel, which further shows intensified sensing response signal. The band structure for the sensing system is shown in Fig. 7c [35]. The potential barriers and electric effect of noble metal have shown by their conduction energy band. The electron flow occurs from sensing material SnO_2 to Au sensitization (catalyst) because Au has lower conduction band bottom than SnO_2 and the work function of Au is higher than semiconducting metal oxide (SnO_2). When LPG is exposed, the LPG molecules react with sensor material, in the chemical reaction and then the electron from lower unoccupied molecular orbital (LUMO) of LPG (reducing gas) transfers to SnO_2 as well as to Au. Which lowers the sensor resistance and hence sensor response increases.

The transient LPG responses of unsensitized SnO_2 at 623 K and Au-sensitized SnO_2 film at 598 K on exposure of 780 ppm LPG are shown in Fig. 8. As the LPG molecule adsorb and react with pre

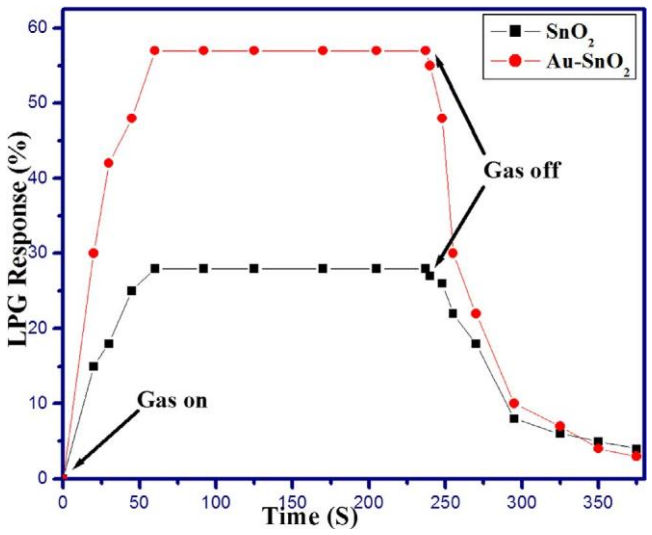

Fig. 8. The transient LPG responses for SnO_2 film at 623 K and Au-sensitized SnO_2 film at 598 K upon exposure to 780 ppm of LPG.

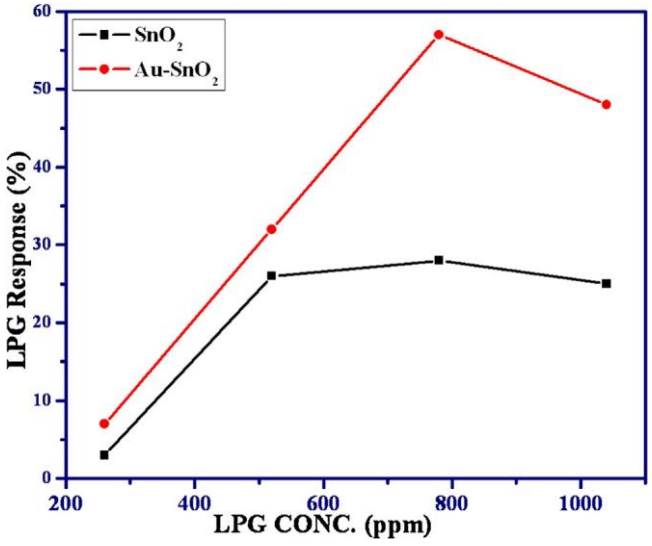

Fig. 9. Response curves of the SnO_2 film at 623 K and Au-sensitized SnO_2 film at 598 K upon exposure of various LPG concentrations.

chemi-adsorbed oxygen species, the gas response increases with time. After a specific time, the LPG response becomes constant due to saturation or equilibrium condition of LPG molecule adsorption with the sensor surface. When sensor system is exposed to an external (open) system the LPG molecules go under desorption which lowers down gas response. The time required for attending maximum LPG response from the time when target LPG introduced in the testing chamber is called as response time. The rapid response time of 60 s is noted for the present sensor. The reproducibility and stability of the Au sensitized SnO_2 sensor was also measured by repeating the experiment many times.

3.6. *LPG concentration effect on sensing*

The effect of LPG concentration on the sensor responses of unsensitized SnO_2 at 623 K temperature and Au-sensitized SnO_2 at 598 K temperature are shown in Fig. 9. The number of LPG molecules react with sensor surface is increased with LPG concentration, which leads to increase in the sensor response. LPG response for both samples is increased with the increase in LPG concentration. Both samples show the highest response at 780 ppm LPG concentration level. The maximum LPG response values noted for unsensitized SnO_2 is 28% and for Au sensitized SnO_2 is 57% for 780 ppm LPG concentration.

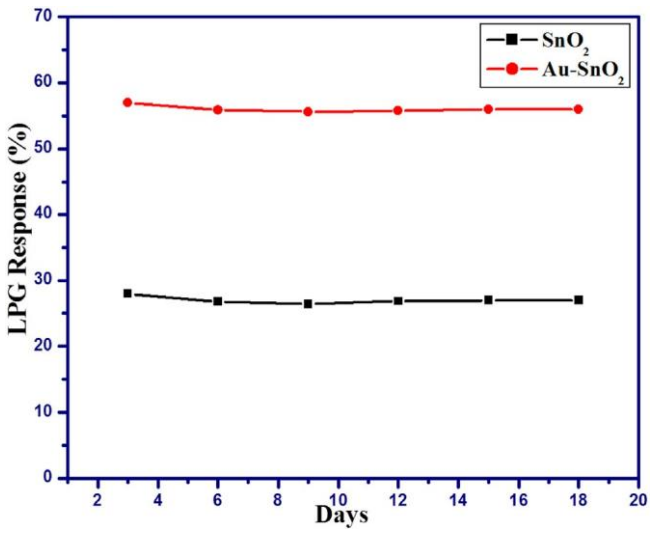

Fig. 10. Stability tests of present sensors.

The stabilities of sensors were checked by testing LPG response multiple times (Fig. 10). Both sensors show approximately good stability. LPG response and operating temperature for Au-SnO_2 sensor are better as compared to previous report [11].

4. Conclusions

In this work, the LPG sensing response of sprayed pristine and Au-sensitized SnO_2 film have been studied and reported. Maximum LPG response found for unsensitized SnO_2 is 28% at 598 K temperature and for Au sensitized SnO_2 is 57% for 780 ppm gas concentration at 598 K operating temperature. The mechanism for enhanced LPG sensing due to Au sensitization is throughly discussed. These sensors exhibit the potential to detect lesser gas concentration than 1000 ppm (Permissible exposure Limit (PEL) for LPG as specified by NIOSH and OSHA standards) with high sensing response. Au sensitized SnO_2 film demonstrates remarkable LPG sensing properties, which makes it as promising high gas response sensor material in partcular when portable sensor device is targeted.

Acknowledgements

Authors are thankful the vice-chancellor Defence Institute of Advanced Technology for (DU) granting financial support and publishing work. SNK would like to thank financial support from "DIAT-DRDO Programme on Nanomaterials" funded by ER-IPR DRDO, Ministry of Defence (ERIP/ER/1003883/M/01/908/2012/D, R&D/1416, dated, 28-3-2012) New Delhi, India. RSM and Mn extend their appreciation to the International Scientific Partnership Program ISPP at King Saud University for funding this research work through ISPP# 0032.

References

[1] F. Lu, Y. liu, M. Dong, X. Wang, Sens. Actuators B 66 (2000) 225–227.
[2] S.W. Choi, A. Katoch, G.J. Sun, S.S. Kim, Sens. Actuators B 181 (2013) 446–453.
[3] A.K. Singh, S.B. Patil, U.T. Nakate, K.V. Gurav, Hindawi Publ. Corp. J. Chem. (2013) 370578–370585.
[4] S.B. Patil, A.K. Singh, J. Mater. Sci. 45 (2010) 5204.

[5] R.R. Salunkhe, D.S. Dhawale, U.M. Patil, C.D. Lokhande, Sens. Actuators B 136 (2009) 39–44.
[6] N. Yamazoe, G. Sakai, K. Shimanoe, Catal. Survey Asia 7 (2003) 63.
[7] A. Chowdhuri, V. Gupta, K. Sreenivas, R. kumar, S. Muzumdar, P.K. Patanjali, Appl. Phys. Lett. 84 (2004) 1180–1182.
[8] D. Haridas, K. Sreenivas, V. Gupta, Sens. Actuators B 133 (2008) 270–275.
[9] S. Chakraborty, A. Sen, H.S. Maiti, Sens. Actuators B 115 (2006) 610–613.
[10] F. Pourfayaz, A. Khodadadi, Y. Mortazavi, S.S. Mohajerzadeh, Sens. Actuators B 108 (2005) 172–176.
[11] U.T. Nakate, R.N. Bulakhe, C.D. Lokhande, S.N. Kale, Appl. Sur. Sci. 371 (2016) 224–230.
[12] P.S. More, R.W. Raut, C.S. Ghuge, Mater. Chem. Phys. 143 (2014) 1278–1281.
[13] T. Samerjai, N. Tamaekong, C. Liewhiran, A. Wisitsoraat, S. Phanichphant, J. Solid State Chem. 214 (2014) 47–52.
[14] U.T. Nakate, P. Patil, R.N. Bulakhe, C.D. Lokhande, S.N. Kale, Mu. Naushad, R.S. Mane, J. Coll. Interfaces Sci. 480 (2016) 109–117.
[15] D.D. Trunga, N.D. Hoaa, P.V. Tonga, N.V. Duya, T.D. Daob, H.V. Chungb, T. Nagaob, N.V. Hieu, J. Hazard. Mater. 265 (2014) 124–132.
[16] S.S. Kim, H.G. Na, S.W. Choi, D.S. Kwak, H.W. Kim, Microelectr. Eng. 105 (2013) 1–7.
[17] W. Jin, S. Yan, W. Chen, S. Yang, C. Zhao, Y. Dai, Mater. Lett. 128 (2014) 362–365.
[18] N. Noor, I.P. Parkin, J. Mater. Chem. C 1 (2013) 984–996.
[19] G.M. Stoian, P.A. Stampe, R.J. Kennedy, Y. Xin, E. Lochner, S.V. Molnár, J. Phys. D: Appl. Phys. 47 (295002) (2014) 1–8.
[20] V. Kumar, A. Jain, D. Pratap, D.C. Agarwal, I. Sulania, V.V.S. Kumar, A. Tripathi, S. Varma, R.S. Chauhan, Adv. Mater. Lett. 4 (6) (2013) 428–432.
[21] G. Battaglin, D. Rosestolato, S. Ferro, A.D. Battisti, Electrocatalysis 4 (2013) 358–366.
[22] S. Ilican, M. Caglar, Y. Caglar, J. Optoelectronics Adv. Mater. 9 (2007) 1414–1417.
[23] D. Perednis, L.J. Gauckler, J. Electroceram. 14 (2005) 103–111.
[24] A.K. Singh, U.T. Nakate, Microwave Synth. Adv. Nanoparticles 2 (2013) 66–70.
[25] A.K. Singh, U.T. Nakate, Microwave Synth. Sci. World J. 7 (2014) 349457.
[26] T.G. Nenov, S.P. Yordanov, Ceram. Sens. Technol. Appl. Technomic Lancaster (1996).
[27] P. Mitra, A.P. Chatterjee, H.S. Maiti, Mater. Lett. 35 (1998) 33–38.
[28] N.J. Dayan, S.R. Sainkar, R.N. Karekar, R.C. Aiyer, Thin Solid Films 325 (1998) 254–258.
[29] K. Arshak, I. Gaidan, Mater. Sci. Eng. B 118 (2005) 44–49.
[30] C. Liewhiran, N. Tamaekong, A. Tuantranont, A. Wisitsoraat, S. Phanichphant, Mater. Chem. Phys. 147 (2014) 661–672.
[31] J.F. McAleer, P.T. Moseley, J.O.W. Norris, D.E. Williams, B.C. Tofield, J. Chem. Soc. Faraday Trans. 1: Phys. Chem. Condens. Phases 84 (1988) 441–457.
[32] W.C. Conner, J.L. Falconer, Chem. Rev. 95 (1995) 759–788.
[33] N. Yamazoe, Y. Kurokawa, T. Seiyama, Sens. Actuators 4 (1983) 283–289.
[34] S. Tian, X. ding, D. Zeng, J. Wu, S. Zhang, C. Xie, RSC Adv. 3 (2013) 11823.